WCCM V
Fifth World Congress on
Computational Mechanics
July 7-12, 2002, Vienna, Austria
Eds.: H.A. Mang, F.G. Rammerstorfer,
J. Eberhardsteiner

A Double-Grid Method for Modeling Microstructure Evolution

J. S. Chen*, H. Lu

Department of Civil & Environmental Engineering
University of California, Los Angeles, Los Angeles, CA90095-1593, USA
e-mail: jschen@seas.ucla.edu

D. Moldovan, D. Wolf

Materials Science Division
Argonne National Laboratory, 9700 S. Cass Ave. Argonne, IL 60439, USA

Key words: grain boundary migration, meshfree method, reproducing kernel approximation, double-gird method

Abstract
The microstructure of materials, i.e. the size, shape and arrangement of grains, determines essentially the material properties such as mechanical strength, toughness, electrical conductivity and magnetic susceptibility. In general the desirable property of materials can be controlled and improved by understanding of microstructure evolution processes in grain growth controlled by grain boundary migration, and grain boundary diffusion. The process of grain growth involves both grain boundary migration (moving interfaces) and topological changes of grain boundary geometry, and it can not be effectively modeled by Lagrangian, Eulerian, or Arbitrary Lagrangian Eulerian finite element method when in addition the stress effect is considered. A double-grid method is proposed for modeling grain boundary migration under stress. In this approach, the material grid carries kinematic and kinetic material variables, whereas the grain boundary grid carries only grain boundary kinematic variables. The material domain is discretized by a reproducing kernel approximation with strain discontinuity enrichment across the grain boundaries. The grain boundaries, on the other hand, are discretized by the standard finite elements. This approach allows modeling of arbitrary evolution of grain boundaries without remeshing.

1 Introduction

Grain growth is the process by which the average grain size in a polycrystalline material increases in time. The evolution of the microstructure during the grain growth takes place via the migration of the grain boundaries towards their centers of curvature, the driving force being provided by the decrease in energy associated with the decrease of the length of the grain boundaries. There have been many experimental and theoretical investigations of grain growth process starting from 1950s. In recent years, various types of computer simulation models have been developed with the aim of simulating the detailed evolution of microstructure during grain growth. These simulation models fall mainly into two classes: probabilistic [1] and deterministic [5, 7, 9, 11, 12].

Probabilistic models are generally of Monte-Carlo type and have their basis in the classical spin models of statistical physics; the most investigated is Potts model [1]. In the Potts model approach grains are subdivided into small-area elements and growth dynamics are simulated by exchange of area elements between grains. Growth takes place as a consequence of the minimization of the internal energy of the system. The exchange step of area elements from one grain to the neighboring grain is carried out using a Monte Carlo algorithm. The advantage of this method is its simplicity and the ease of its implementation in two and three-dimensional systems. However, in this method the origin of the stochastic aspect is not clear, nor is the relation between the Monte Carlo time step and the physical time.

In the deterministic models, the motion of grain boundaries is followed by time integration of their position assuming the normal velocity of the grain boundary to be proportional to the boundary curvature. A purely deterministic approach was proposed first by Fullman [8] and is referred to as "vertex model". Later, this was improved by Soares et al. [12] and Kawasaki et al. [9] assuming straight grain boundaries, and by Frost et al. [7], Cocks and Gill [5], and Weygand et al. [15] by extending it to curved grain boundaries. Using the theoretical approach of Needleman and Rice [11] based on a variational principle for dissipative systems, Cocks and Gill [5] have proposed a new method to simulate curvature-driven grain growth. Their modification describes the rate of power dissipation due to the competition between the reduction in the grain boundary energy and the viscous drag during grain boundary migration. Moreover, the grain boundaries are discretized using finite elements.

When a polycrystalline microstructure is subjected to an externally applied stress, an additional driving force, besides that resulting from the grain boundary curvature, has to be considered. This is due to the elastic anisotropy of the grains comprising the microstructure, which in general store different amounts of elastic energies. Our focus in this study is to investigate the grain growth in the presence of both curvature driven and stress induced grain boundary migration.

In this work, we introduce a variational equation based on the balance of energies associated with grain boundary surface tension and curvature, elastic strain energy, and the elastic strain energy difference due to anisotropy between adjacent grains. This reflects the coupling of elastic deformation of grains with grain boundary migration and thus necessitates the discretization of grain boundaries and grain domains. Using finite element method to study the migration of grain boundaries leads to a severe mesh distortion in each grain, and the topological changes of grain structures further demand a complete remeshing. To address the above mentioned issues, a double-grid method is proposed. The elastic deformation of grains is modeled by a reproducing kernel discretization with built-in strain

discontinuities along the grain boundaries [3, 4, 14], whereas the migration kinematics of discretized grain boundaries is modeled using the standard finite element approximation.

The layout of this paper is as follows. Grain growth kinematics and the geometry of polycrystalline system are briefly reviewed in Section 2. In Section 3, the variational formulation for boundary migration under stress is presented. The doubled-grid discretization and formulation for grain boundary and material domains are introduced in Section 4. Section 5 demonstrates that the evolution of grain growth can be effectively simulated without any remeshing through numerical examples.

2 Grain Growth Kinematics and Polycrystalline Geometry

2.1 Grain Growth Kinematics

In general, the grain boundaries migrate at a wide range of velocities, which depend on the magnitude of both the driving force and the grain boundary mobility (dependent on temperature, and impurities concentration). Using a simplified model, Burke and Turnbull [2] proposed a parabolic relationship for the grain growth kinetic.

The driving force f_c due to the surface curvature (the capillarity effect) is

$$f_c = \gamma(\theta)\left(\frac{1}{R_1} + \frac{1}{R_2}\right) \tag{1}$$

where $\gamma(\theta)$ is the surface tension (the boundary energy per unit area) which in general dependents on the grain-boundary misorientation θ, and R_1 and R_2 are the principal radii of the surface curvature.

Assuming that the only forces acting on a grain boundary are those given by Eq.(1) and that $\gamma(\theta)$ is constant for all boundaries, the growth process is characterized by the parabolic equation:

$$\bar{R}^n(t) - \bar{R}^n(0) = kt \tag{2}$$

where n takes the value of 2 and is known as the grain growth exponent, $\bar{R}(t)$ is the mean grain radius at time t, and k is a constant. The grain growth exponent is one of the most important characteristics of the growth and the experimental value ranges from n=2 to n=4.

In general at small grain sizes the most significant driving force for grain boundary migration is the surface tension. However, at larger grain sizes and in the presence of strain energy, additional driving forces [6] due to the difference in elastic strain energies in the volumes of neighboring grains, may also play a key role in grain boundary migration. For instance, this driving force f_e can be expressed as:

$$f_e = \frac{|\Delta U|}{\Delta V} \tag{3}$$

where ΔU is the difference in the strain energy stored in volume ΔV between adjacent grains, and ΔV is the volume through which the grain boundary segment has swept during a migration step.

2.2 Topology of Polycrystalline Geometry

The geometry of a 2D polycrystalline material is determined by the arrangement of the fundamental elements such as vertices, edges and faces as shown in Fig. 1. These elements obey the Euler relation:

$$F - E + V = 1 \tag{4}$$

where F, E, and V are the numbers of faces, edges and vertices. Although any number of edges can join in a vertex, the threefold vertices are the one favored energetically in 2-D polycrystalline systems, and it follows

$$3V = 2E = \bar{n}F \tag{5}$$

where $\bar{n}$ is the mean number of vertices per face (grain). For a system with a large number of grains $N \gg 1$, this implies $\bar{n} = 6$.

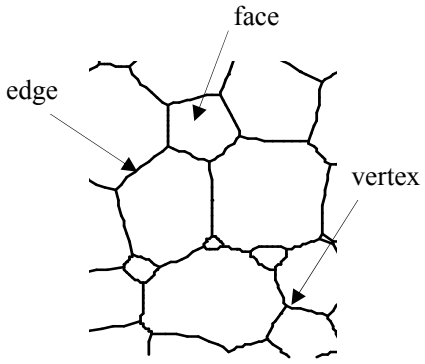

Figure 1: 2-D grain structure

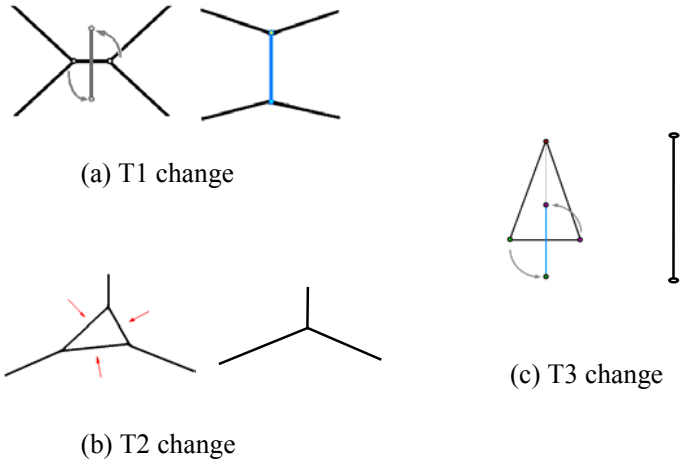

(a) T1 change

(b) T2 change

(c) T3 change

Figure 2: Topological changes of grain boundaries

In 2D, unless the microstructure consists of a regular array of hexagons, grain growth is inevitable. According to Eq. (5), each grain disappearance is accompanied by vanishing of two vertices and three edges. Moreover, for a system with isotropic grain boundary properties, the von Neumann [13] relation predicts that any grain with more than 6 edges will grow, while those having less 6 edges will shrink. The topology of the system evolves continuously during growth. In order to provide solutions for the necessary topological transformations during growth, typical topological transformations have been implemented. These are T1, T2 and T3 topological changes as shown in Fig. 2.

3 Variational Formulation

As the formal basis for this study we use the variational principle for dissipative systems originally formulated by Needleman and Rice [11] for grain boundary and surface diffusion in the context of void growth. Latter this was adapted for grain boundary migration studies by Cocks and Gill [5]. Here we extend this formalism by incorporating additional terms for grain boundary migration under the effect of stress. Due to the flexibility of the variational approach it is straightforward to add additional terms to the variational functional describing different phenomena such as grain boundary diffusion and surface diffusion. Consider a two-dimensional domain Ω with a grain boundary network Γ_{gb}, external boundary Γ, and is subjected to an external traction as shown in Fig. 3.

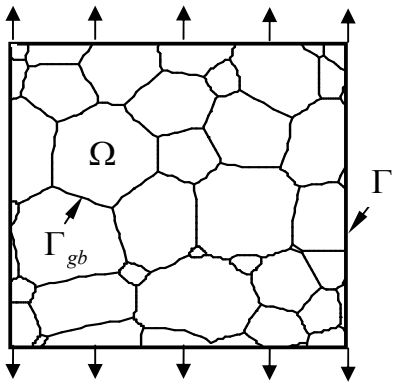

Figure 3: Problem model

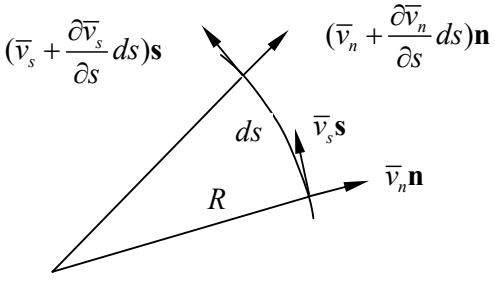

Figure 4: A segment of grain boundary

We start with a virtual grain boundary migration with a virtual velocity $\overline{v}_n$ normal to the grain boundary and a virtual velocity $\overline{v}_s$ along the arc length of the boundary. The positive normal direction is defined as the normal direction pointing outward with respect to the curvature center of the surface as shown in Fig. 4. The virtual rate of energy dissipation associated with a virtual grain boundary migration velocity $\overline{\boldsymbol{v}}$ is

$$\delta\dot{W}_1 = \int_{\Gamma_{gb}} f_c \delta\overline{v}_n d\Gamma_{gb} \tag{6}$$

Due to the velocities $\overline{v}_n$ and $\overline{v}_s$, as shown in Fig. 4, the rate of elongations per unit length of the grain boundary can be calculated as

$$\delta\dot{\varepsilon}_s = \frac{\delta v_n}{R} + \frac{\partial \delta v_s}{\partial s} \tag{7}$$

where R is grain boundary radius of curvature. Therefore the rate of virtual work done by the grain boundary tension reads

$$\delta\dot{W}_2 = \int_{\Gamma_{gb}} \gamma\delta\dot{\varepsilon}_s ds = \int_{\Gamma_{gb}} \gamma(\frac{\delta v_n}{R} + \frac{\partial\delta v_s}{\partial s})ds \tag{8}$$

In a system in which there is a variation in the material elastic properties of any two adjacent grains, the strain energy density in the two regions on the opposite side of a grain boundary is in general different. Therefore, when an external stress is considered, besides the capillary force, there is an additional contribution to the driving force acting on a grain boundary due to the discontinuities in the strain energy density distribution across the boundary. As shown in Fig. 5, the gain of virtual rate of strain energy in response to the virtual velocity of the grain boundary $\delta\overline{v}_n$ can be written as

$$\delta\dot{W}_3 = \int_{\Gamma_{gb}} \frac{1}{2}\boldsymbol{\sigma} : (\boldsymbol{\varepsilon}^+ - \boldsymbol{\varepsilon}^-)\delta\overline{v}_n d\Gamma \tag{9}$$

where $\boldsymbol{\varepsilon}^+$ is the strain in the grain that gains virtual area $\delta\overline{v}_n d\Gamma$ (grain A), and $\boldsymbol{\varepsilon}^-$ is the strain in the grain located on the other side of the grain boundary (grain B).

The principle of virtual work of the above effects reads:

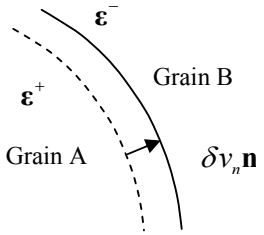

Figure 5: Strain energy change due to grain boundary migration

$$\int_{\Gamma_{gb}} \gamma\left(\frac{\partial \delta \overline{v}_s}{\partial s} + \frac{\delta \overline{v}_n}{R}\right) ds + \int_{\Gamma_{gb}} f_c \delta \overline{v}_n ds + \int_{\Gamma_{gb}} \frac{1}{2} \boldsymbol{\sigma} : (\boldsymbol{\varepsilon}^+ - \boldsymbol{\varepsilon}^-) \delta \overline{v}_n d\Gamma$$
$$+ \int_{\Omega} \delta\left(\frac{1}{2} \dot{\varepsilon}_{ij} \sigma_{ij}\right) d\Omega - \int_{\Gamma_h} \delta v_i h_i d\Gamma - \int_{\Omega} \delta v_i b_i d\Gamma = 0 \tag{10}$$

The first two terms in Eq. (10) correspond to the rate of grain boundary network energy change and the rate of energy dissipated by the migration of grain boundaries. The third term gives the rate of elastic energy change due to grain boundary migration while the fourth term quantifies the rate of energy change of the elastic energy due to the change in the stress and strain field. The last to terms in Eq. (10) are due to the rate of work done by the external forces (bulk and surface traction). In addition to this a creep law is considered for each grain as

$$\sigma_{ij} = C_{ijkl} \dot{\varepsilon}_{kl} \tag{11}$$

$$\dot{\varepsilon}_{ij} = \frac{1}{2}\left(\frac{\partial v_i}{\partial x_j} + \frac{\partial v_j}{\partial x_i}\right) \tag{12}$$

v_i is material velocity, h_i is surface traction, b_i is body force and Γ_h is boundary with surface traction. The viscoelastic tensor C_{ijkl} is generally anisotropic describing the crystallographic orientation of grain.

Assuming the normal velocity $\overline{v}_n$ of grain boundary is proportional to the driving force, i.e.

$$\overline{v}_n = m f_c \tag{13}$$

where m is grain boundary mobility associated with driving force f_c, Eq. (10) reduces to

$$\int_{\Gamma_{gb}} \gamma\left(\frac{\partial \delta \overline{v}_s}{\partial s} + \frac{\delta \overline{v}_n}{R}\right) ds + \int_{\Gamma_{gb}} \frac{\overline{v}_n}{m} \delta \overline{v}_n ds + \int_{\Gamma_{gb}} \frac{1}{2} \boldsymbol{\sigma} : (\boldsymbol{\varepsilon}^+ - \boldsymbol{\varepsilon}^-) \delta \overline{v}_n d\Gamma$$
$$+ \int_{\Omega} \dot{\varepsilon}_{ij} C_{ijkl} \delta \dot{\varepsilon}_{kl} d\Omega - \int_{\Gamma_h} \delta v_i h_i d\Gamma - \int_{\Omega} \delta v_i b_i d\Gamma = 0 \tag{14}$$

4 A Double-grid Formulation

Grain boundary velocity $\overline{\boldsymbol{v}}$ and material velocity $\boldsymbol{v}$ are the two primary variables involved in the formulation of this physical problem. As shown in Fig. 6, the material domain is discretized by introduction of material points carrying material velocity $\boldsymbol{v}$, whereas the grain boundary is discretized by defining the grain boundary points carrying grain boundary velocity $\overline{\boldsymbol{v}}$. In this approach, the material velocity is approximated by a reproducing kernel approximation with strain discontinuity along material interface [4, 14]. The grain boundary velocity is approximated by the standard finite element shape function, i.e.,

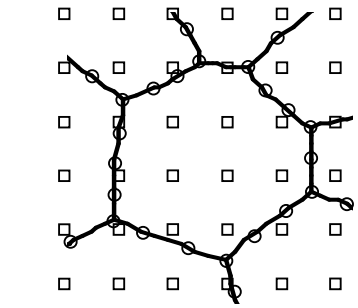

Figure 6: Double grid discretization

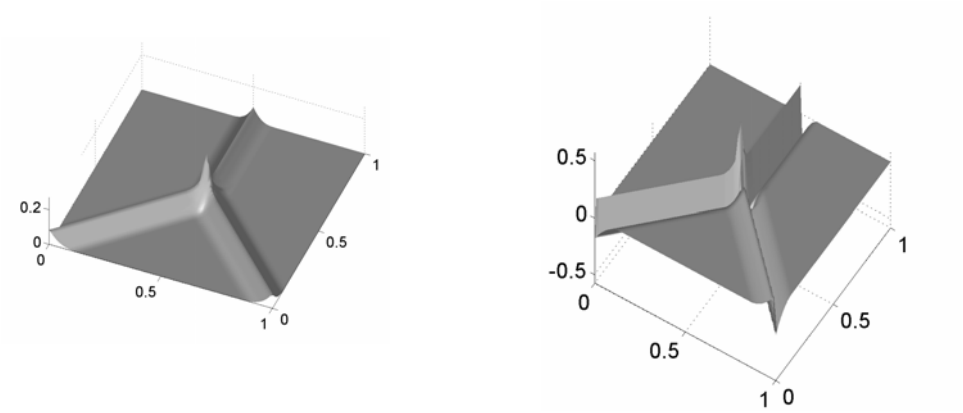

Figure 7: Interface enrichment function and its derivatives along the normal direction of the grain boundaries

$$v_i = \sum_{I=1}^{NPm} \Psi_I(\boldsymbol{x}) \upsilon_{iI} \tag{15}$$

$$\overline{v}_i = \sum_{I=1}^{NPgb} N_I(s) \overline{\upsilon}_{iI} \tag{16}$$

where NPm is the number of material points, NPgb is the number of grain boundary points, $N_I(s)$ is the 1-dimensional shape function defined along the grain boundary using grain boundary coordinate s, and $\Psi_I(\boldsymbol{x})$ is the reproducing kernel shape function defined in the 2-dimensional material domain as follows

$$\Psi(\boldsymbol{x}) = \hat{\Psi}(\boldsymbol{x}) + \overline{\Psi}(\boldsymbol{x}) \tag{17}$$

In Eq. (17), $\hat{\Psi}(\boldsymbol{x})$ is the interface enrichment function employed to introduce derivative discontinuity along the grain boundary as shown in Fig. 7, and $\bar{\Psi}(\boldsymbol{x})$ is the reproducing kernel function introduced to impose completeness of the approximation. Following the procedures described in [4, 14] the reproducing kernel function is expressed as

$$\bar{\Psi}_I(\boldsymbol{x}) = \boldsymbol{H}^T(\boldsymbol{x}-\boldsymbol{x}_I)\boldsymbol{M}^{-1}(\boldsymbol{x})[\boldsymbol{H}(\boldsymbol{0}) - \sum_{I=1}^{NPm}\hat{\Psi}(\boldsymbol{x})\boldsymbol{H}(\boldsymbol{x}-\boldsymbol{x}_I)]\Phi_a(\boldsymbol{x}-\boldsymbol{x}_I) \tag{18}$$

$$\boldsymbol{H}^T(\boldsymbol{x}-\boldsymbol{x}_I) = [1, x-x_I, y-y_I] \tag{19}$$

$$\boldsymbol{M}(\boldsymbol{x}) = \sum_{I=1}^{NPm}\boldsymbol{H}(\boldsymbol{x}-\boldsymbol{x}_I)\boldsymbol{H}^T(\boldsymbol{x}-\boldsymbol{x}_I)\Phi_a(\boldsymbol{x}-\boldsymbol{x}_I) \tag{20}$$

where $\Phi_a(\boldsymbol{x}-\boldsymbol{x}_I)$ is the kernel function with support size "a".

For the typical grain boundary element shown in Fig. 8, the corresponding approximation is obtained by following equations.

$$\bar{\boldsymbol{v}}^h = \begin{bmatrix}\bar{v}_1^h \\ \bar{v}_2^h\end{bmatrix} = \begin{bmatrix}\sum_I N_I\bar{\upsilon}_{I1} \\ \sum_I N_I\bar{\upsilon}_{I2}\end{bmatrix} = \sum_I \boldsymbol{N}_I\bar{\boldsymbol{\upsilon}}_I \tag{21}$$

$$\boldsymbol{N}_I = \begin{bmatrix}N_I & 0 \\ 0 & N_I\end{bmatrix} \tag{22}$$

$$\bar{\boldsymbol{\upsilon}}_I = \begin{bmatrix}\bar{\upsilon}_{I1} \\ \bar{\upsilon}_{2I}\end{bmatrix} \tag{23}$$

$$\bar{v}_n = [e_{nx}, e_{ny}]\begin{bmatrix}\bar{v}_1 \\ \bar{v}_2\end{bmatrix} = \boldsymbol{R}_n\bar{\boldsymbol{v}} = \sum_I \boldsymbol{R}_n\boldsymbol{N}_I\bar{\boldsymbol{\upsilon}}_I \tag{24}$$

$$\boldsymbol{R}_n = [e_{nx}, e_{ny}] \tag{25}$$

$$\bar{v}_s = [e_{sx}, e_{sy}]\begin{bmatrix}\bar{v}_1 \\ \bar{v}_2\end{bmatrix} = \boldsymbol{R}_s\bar{\boldsymbol{v}} = \sum_I \boldsymbol{R}_s\boldsymbol{N}_I\bar{\boldsymbol{\upsilon}}_I \tag{26}$$

$$\boldsymbol{R}_s = [e_{sx}, e_{sy}] \tag{27}$$

where $\mathbf{e}_n$ and $\mathbf{e}_s$ are of normal and tangential unit vectors, respectively, shown in Fig. 8.

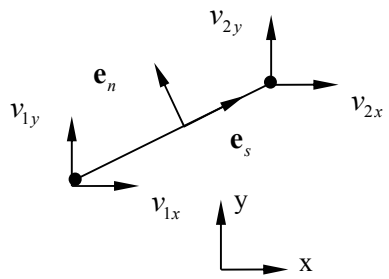

Figure 8: Typical grain boundary element

The matrix equations are obtained by substituting previous equations into Eqn. (14) to yield

$$\boldsymbol{K}\boldsymbol{\upsilon} = \boldsymbol{f}^{ext} + \boldsymbol{f}^{bd} \tag{28}$$

$$\boldsymbol{C}^{gb}\overline{\boldsymbol{\upsilon}} = -\boldsymbol{f}^{gb} - \boldsymbol{f}^{st} \tag{29}$$

where

$$\boldsymbol{K}_{IJ} = \int_{\Omega} \boldsymbol{B}_I^T \boldsymbol{C} \boldsymbol{B}_J d\Omega \tag{30}$$

$$\boldsymbol{B}_I = \begin{bmatrix} \Psi_{I,x} & 0 \\ 0 & \Psi_{I,y} \\ \Psi_{I,y} & \Psi_{I,x} \end{bmatrix} \tag{31}$$

$$\mathbf{C} = \begin{bmatrix} C_{1111} & C_{1122} & C_{1112} \\ C_{2211} & C_{2222} & C_{2212} \\ C_{1211} & C_{1222} & C_{1212} \end{bmatrix} \tag{32}$$

$$\boldsymbol{f}_I^{ext} = \int_{\Gamma_h} \Psi_I \boldsymbol{h} d\Gamma \tag{33}$$

$$\boldsymbol{f}_I^{bd} = \int_{\Omega} \Psi_I \boldsymbol{b} d\Omega \tag{34}$$

$$\boldsymbol{f}_I^{gb} = \sum_{i=1}^{Ngb} [\gamma \boldsymbol{N}_I^T \boldsymbol{R}_s^T]\Big|_{s_i^l}^{s_i^l} + \sum_{i=1}^{Ngb} \int_{\Gamma_i^{gb}} \gamma \frac{\boldsymbol{N}_I^T \boldsymbol{R}_n^T}{R} d\Gamma \tag{35}$$

$$\boldsymbol{C}_{IJ}^{gb} = \sum_{i=1}^{Ngb} \int_{\Gamma_i^{gb}} \frac{1}{m} \bar{\boldsymbol{N}}^T \boldsymbol{R}_n{}^T \boldsymbol{R}_n \bar{\boldsymbol{N}} d\Gamma \tag{36}$$

$$\bar{\boldsymbol{N}} = \begin{bmatrix} N_1 & N_2 \end{bmatrix} \tag{37}$$

$$\boldsymbol{f}_I^{st} = \sum_{i=1}^{Ngb} \int_{\Gamma_i^{gb}} \frac{1}{2} \boldsymbol{\sigma} : (\boldsymbol{\varepsilon}^+ - \boldsymbol{\varepsilon}^-) \boldsymbol{N}_I^T \boldsymbol{R}_n^T d\Gamma \tag{38}$$

5 Numerical examples

First, the focus of our study is on the grain growth by grain boundary migration only. Two seven-side and two five-side grains were introduced at the center of a perfect hexagonal array as shown in Fig. 9 (a). The elastic properties of all the grains comprising the microstructure are assumed to be isotropic. The presence of the topological imperfections in the grain network triggers the time evolution of the microstructure; the driving force being the reduction of the free energy of the grain boundary network. As the time progresses the grain boundary migration via topology changes generates additional grains that are not 6 sided. In agreement with the von Newman relation [10, 13], the grains with less than 6 edges continue to shrink and eventually disappear while those having more than 6 sides continue to grow. The time evolution of the microstructure is shown in Figs. 9 (b)-(f).

Next, the focus of our study is on the coupling between curvature-driven and stress induced grain boundary migration. A network of uniform hexagonal grains, with a central one whose elastic material property is different from the others, (as shown in Figs. 10 and 11) is subjected to a tensile stress in the vertical direction. In the first case, the Young's modulus of the center grain is greater than that of the other grains. The evolution of microstructure is shown in the six snapshots of Fig. 10. Interestingly, although all of the grains in the microstructure have the same topology (six sided) the microstructure is unstable to grain growth. This instability is due to the additional driving force acting on the boundaries surrounding the center grain resulting from the different elastic energy stored in the center grain and the surrounding ones. The center grain has a lower energy density. Several T1 topological changes on the grain boundaries of grains surrounding the center one give rise to a grains with less than 6 edges therefore this further promotes its growth (see central grain in Fig. 10). In the end this continuous evolution results in a central grain that occupies most of the domain.

In the second case, a central grain with smaller Young's modulus is introduced. In this case the center grain has a higher elastic energy density compared with the neighboring ones. Therefore at the initial stage, this grain shrinks as shown in Fig. 11 in order to reduce the total strain energy of the system. After several T1 and T3 topological changes, the central grain disappears and leads to an unstable microstructure where several grains have less than 6 edges and one with more than 6 edges. The one grain with more than 6 edges continues to grow whereas the surrounding grains with less than 6 edges keep on reducing their sizes and eventually disappear.

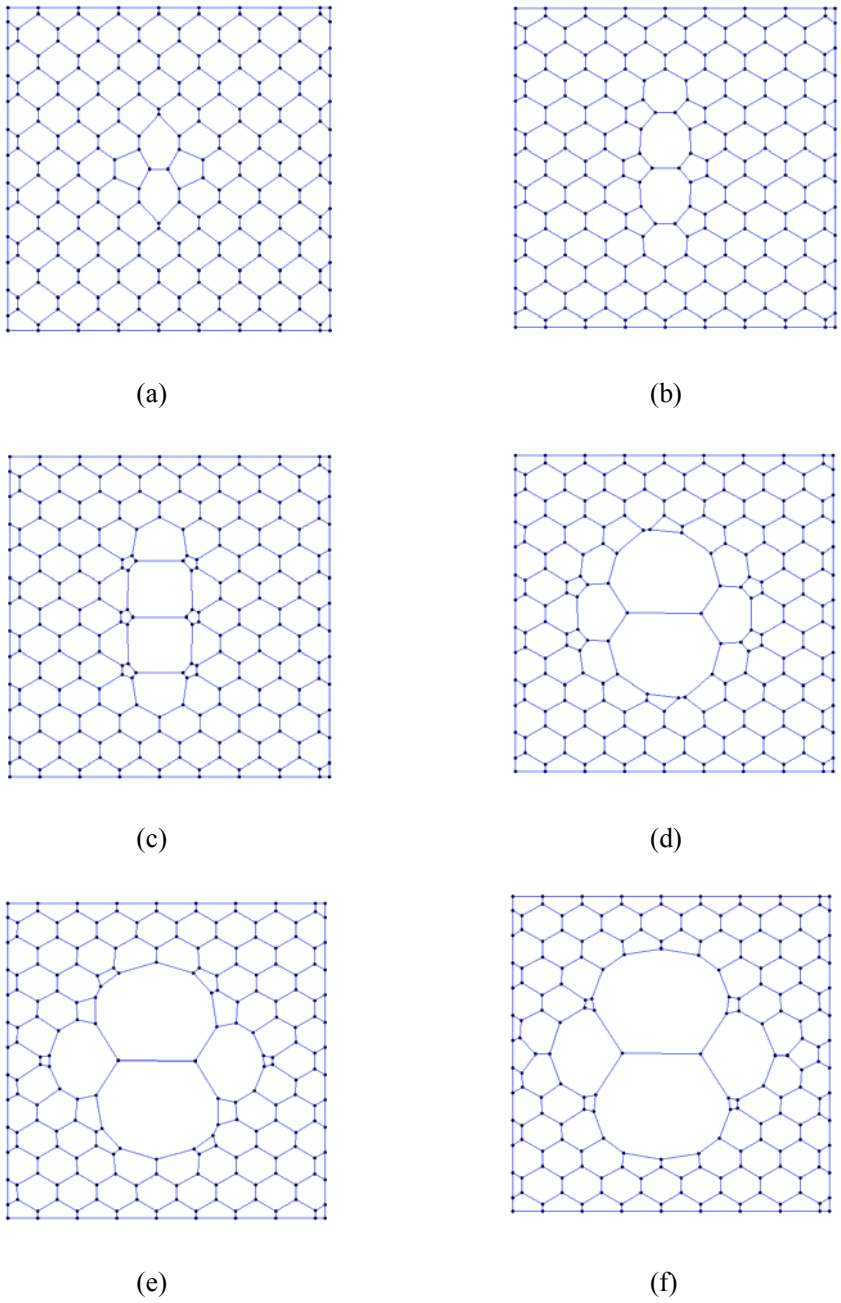

Figure 9: Grain growth in regular hexagonal structure with imperfection in the center

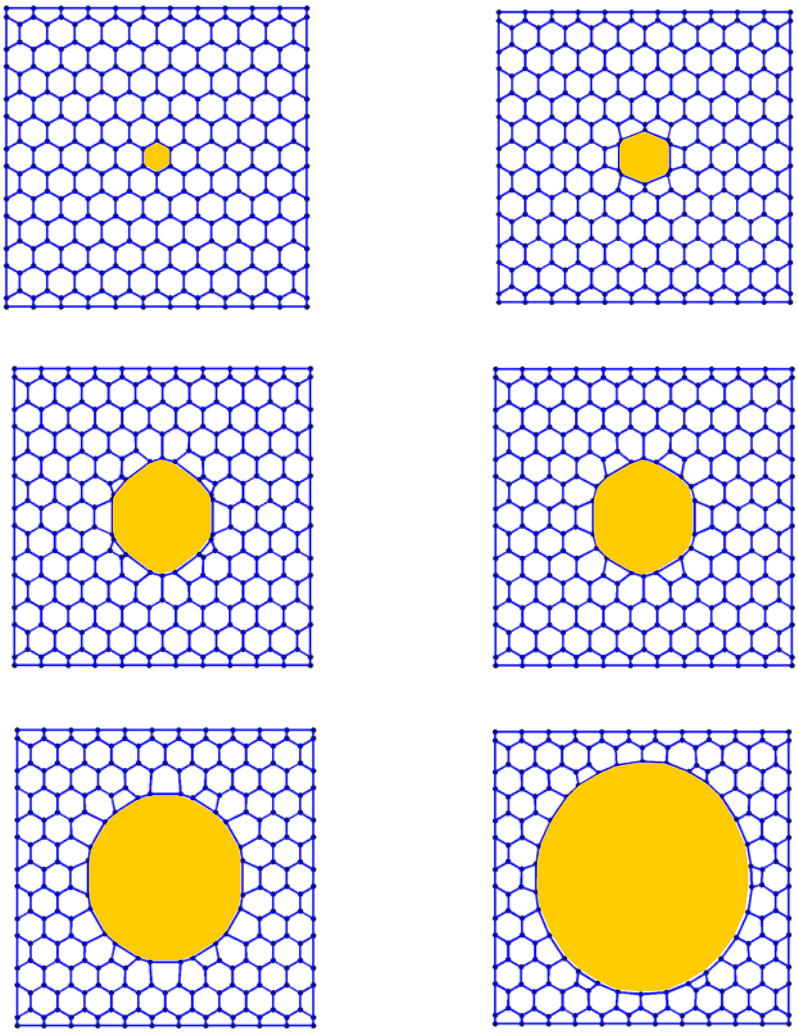

Figure 10: Imperfection with stiffer grain

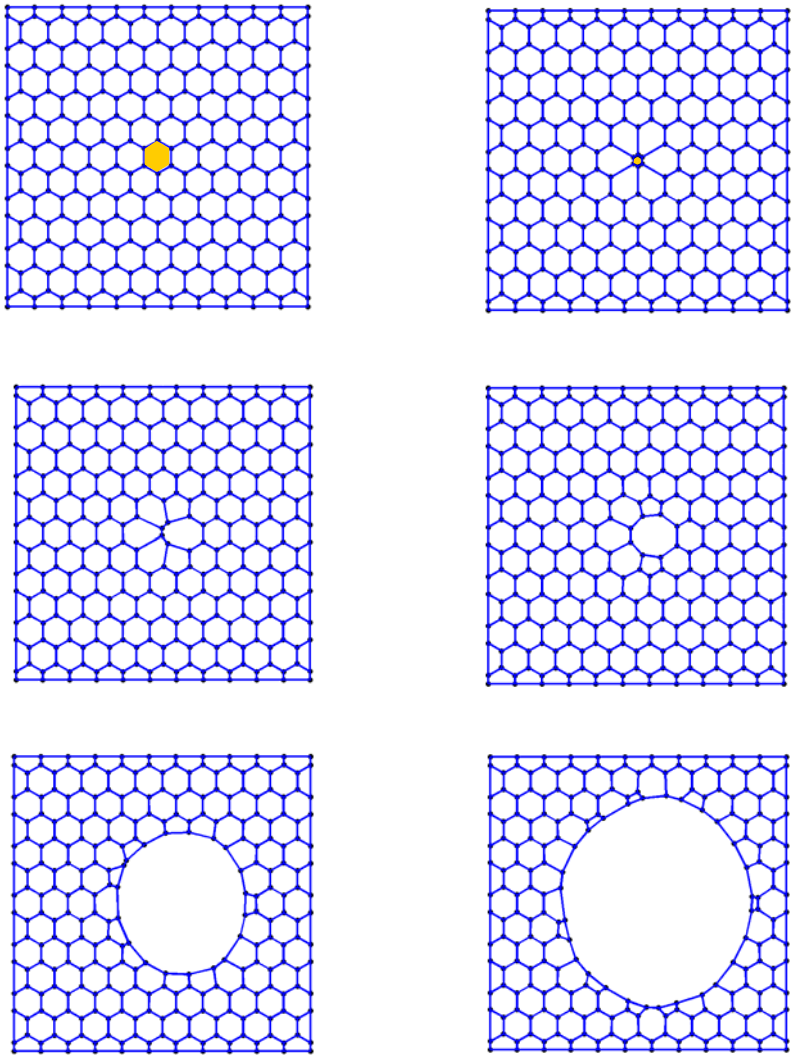

Figure 11: Imperfection with softer grain

6 Conclusion

A variational formulation and a double-grid discretization method for modeling grain growth and boundary migration are introduced in this work. The material velocity field inside each grain is interpolated by a reproducing kernel function defined on a background grid. The grain boundary migration velocity, on the other hand, is interpolated by a set of finite element shape functions defined on the grain boundaries. The new variational formulation takes into account the strain energy effects

on the evolution of the microstructure during grain growth, and the double-grid approach allows the modeling of microstructure evolution in polycrystalline materials without the tedious remeshing.

Acknowledgements

The support of this work by NSF/DARPA OPAAL Program under grant DMS 98-74015 to UCLA is greatly acknowledged. D.M and D.W were supported by the U.S. Department of Energy, Office of Science, under Contract W-31-109-Eng-38.

References

[1] M. P. Anderson, D. J. Srolovitz, G. S. Grest, and P. S. Sahni, *Computer Simulation of Grain Growth-I. Kinetcis,* Acta Metall., 32, (1984), 783-791.

[2] J.E. Burke, and D. Turnbull, Progress in Materials Physics, 3, (1952), 220.

[3] J. S. Chen, W. Han, Y. You, X. Meng, *Reproducing Kernel Interpolation without Finite Element Enrichment*, in review, International Journal for Numerical Methods in Engineering (2002).

[4] J. S. Chen, C. Pan, , C. T. Wu and W. K. Liu, *Reproducing Kernel Particle Methods for Large Deformation Analysis of Nonlinear Structures,* Computer Methods in Applied Mechanics and Engineering, 139, (1996), 195-227

[5] A. C. F. Cocks, and S. P. A. Gill, *A Variational Approach to Two Dimensional Grain Growth-I. Theory,* Acta Mater., 44, (1996), 4765-4775.

[6] A. C. F. Cocks, S. P. A. Gill, and J. Pan, *Modeling Microstructure Evolution in Engineering Materials,* Advances in Applied Mechanics, 36, (1999), 81-162

[7] H. J. Frost, C. V. Thompson, C. L. Howe, and Junho Whang, *A Two-Dimensional Computer Simulation of Capillarity-Driven Grain Growth: Preliminary Results*, Scripta Metallugica, 22, (1988), 65-70.

[8] R. L. Fullman, Metal Interface, American Society for Metals, (1952), 179-259.

[9] K. Kawasaki, T. Nagai, and K. Nakashima, *Vertex Models for Two-Dimensional Grain Growth,* Philosophical Magazine B, 60, (1989), 399-421.

[10] D. Moldovan, D. Wolf, S. R. Phillpot ,and A. J. Haslam, Philosophical Magazine A, (2002), (in press).

[11] A. Needleman, and J. R. Rice, *Plastic Creep Flow Effects in the Diffusive Cavitation of Grain Boundaries,* Acta Metall., 28, (1980), 1315-1332.

[12] A. Soares, A. C. Ferro, and M. A. Fortes, *Computer Simulation of Grain Growth in a Bidimensional Polycrystal,* Scripta Metallurgical, 19, (1985), 1491-1496.

[13] J. von Neumann, Metal interfaces (Metals Park, Ohio: American Society for Metals), (1952), 108.

[14] D. Wang, and J. S. Chen, *Homogenization of Magnetostrictive Particle-Filled Elastomers using Meshfree Method with Interface Discontinuity,* Invited for publication in special issue of Journal of Finite Element Analysis and Design (Finalist of Robert Melosh student paper competition) (2002).

[15] D. Weygand, and Y. Brechet, *A Vertex Dynamics Simulation of Grain Growth in Two Dimensions,* Philosophical Magazine B, 78, (1998), 329-352.